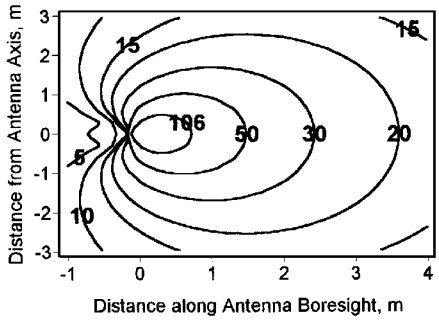

Fig. 3 Electric fields (V/m) produced by S-band low-gain antenna.

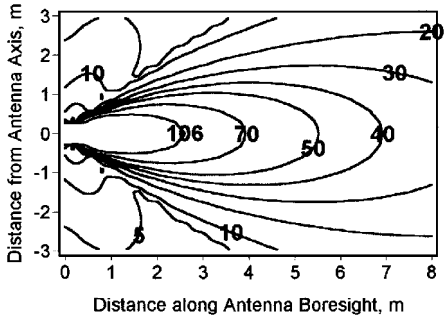

Fig. 4 Electric fields (V/m) produced by S-band high-gain antenna.

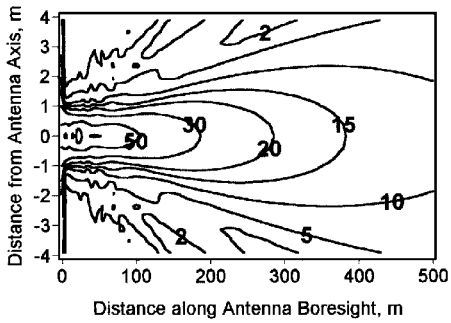

Fig. 5 Electric fields (V/m) produced by Ku-band antenna.

of $-120 \le \theta \le 120$ deg and $-60 \le \phi \le 60$ deg. The S-band antenna transmit frequency is 2.265 GHz, and the antennas are located at (−2.53, 0.09, −14.26) m, (0.26, 8.14, −4.19) m, and (0.26, −9.19, −4.19) m referenced to the ISS coordinate system. The peak gain is 16 dB. The maximum transmitted power referenced at the power amplifier output is 40 W. The nominal cable loss between the power amplifier output and antenna is 1 dB at the minimum operation temperature.[3] The aperture integration technique was used to compute the electric fields for this antenna.[4] The conical horn antenna model was validated by measured far-field S-band antenna radiation patterns.

Figure 4 shows the electric fields (volts per meter) produced by the S-band high-gain antenna. The radiated energy is spread mostly within a cone region. The keep-out zone, in which the electric fields are greater than the maximum permitted 106-V/m exposure level, for the EMU electronics is approximately a cylindrical region of 1 m in diameter and 2.6 m in length, extending forward from the antenna.

The Ku-band antenna transmit frequency is 15 GHz and is located at (−4.81, −4.17, −3.56) m in the ISS coordinate system. The peak gain is 48.4 dB. The maximum transmitted power referenced at the power amplifier output is 10 W. The nominal cable loss is 1 dB at the minimum operation temperature.[3] In the field computations for the Ku-band reflector antenna, the geometrical theory of diffraction (GTD) is used.[5] The GTD-computed field intensities were validated by the anechoic-chamber-measured, far-field Ku-band antenna radiation patterns.

Figure 5 shows the electric fields (volts per meter) produced by the Ku-band high-gain antenna. For a range distance less than 100 m from the aperture, the radiated energy is mainly confined within the aperture projected cylinder. The alternate electric field peaks and valleys of the Fresnel zone phenomenon are observed in close range distances less than 40 m. The rf exposure limit for the EMU electronics at the Ku-band frequency is 20 V/m. The keep-out zone, in which the electric fields are greater than the maximum permitted 20-V/m exposure level, is approximately a cylindrical region of 2.4 m in diameter and 290 m in length, extending forward from the antenna.

Conclusions

The electric fields around the various space station transmitting antennas are computed and presented. This information is important in assessing personnel and electronic equipment rf exposure hazards and is useful for the users of the space station who are designing scientific experiment payloads to be operated in the space station environment. As an example, the keep-out zones in which the electric fields exceed the specified maximum permitted rf exposure to the EMU electronics on the space suit were determined. Similarly, keep-out zones for other equipment can be determined using information presented in this Note.

References

[1] Murphy, G. B., and Cutler, W. D., "Orbiter Environment at S- and Ku-Band Frequencies," *Journal of Spacecraft and Rockets*, Vol. 25, No. 1, 1988, pp. 81–87.

[2] Hwu, S. U., Wilton, D. R., and Rao, S. M., "Electromagnetic Scattering and Radiation by Arbitrary Conducting Wire/Surface Configurations," *IEEE International Antennas and Propagation Symposium Digest*, Inst. of Electrical and Electronics Engineers, Piscataway, NJ, 1988, pp. 890–893.

[3] Loh, Y. C., and Adkins, A. A., "International Space Station (ISS), United States On-Orbit Segments (USOS), Circuit Margin Data Book," NASA Johnson Space Center, TR JSC-27437, Revision A, Dec. 1996.

[4] Clarricoats, P. J. B., and Saha, P. K., "Propagation and Radiation Behaviour of Corrugated Feeds. Part II—Corrugated Conical Horn Feed," *Proceedings of IEE*, Vol. 118, No. 9, 1971, pp. 1177–1186.

[5] Lee, S. H., and Rudduck, R. C., "Aperture Integration and GTD Techniques Used in the NEC Reflector Antenna Code," *IEEE Transactions on Antennas and Propagation*, Vol. 33, No. 2, 1985, pp. 189–194.

A. C. Tribble
Associate Editor

Efficient Approach for International Space Station Global Positioning System Multipath Analysis

Shian U. Hwu*
Lockheed Martin Space Mission Systems and Services, Houston, Texas 77258
and
Robert J. Panneton† and Susan F. Gomez‡
NASA Johnson Space Center, Houston, Texas 77258

Introduction

THE international space station (ISS) is very large in terms of physical and electrical size and is a very complex space vehicle, as shown in Fig. 1. The solar panels and thermal radiators are rotated dynamically to maintain preferential orientation with respect to the sun. The Global Positioning System (GPS) antennas have to track the GPS satellites in a wide-field-of-view region and will encounter multipath interference from the ISS structures. Multipath is an important error source for attitude determination.[1,2]

Received May 7, 1997; revision received July 25, 1997; accepted for publication Aug. 1, 1997.

*Principal Engineer, Communication, Tracking Analysis and Test Section, MC: C02, 2400 NASA Road One. Senior Member AIAA.

†Project Engineer, Avionics Test and Analysis Branch, MC: EV413.

‡Project Engineer, Guidance and Navigation Branch, MC: EG4.

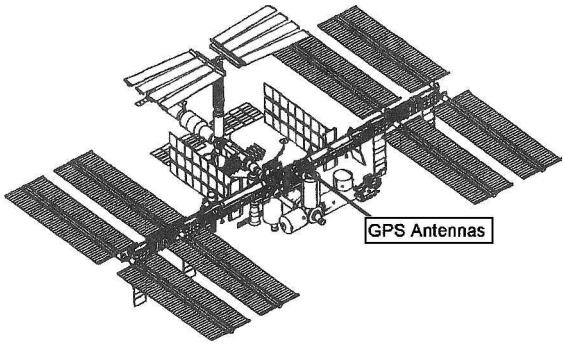

Fig. 1 International space station configuration. Design analysis cycle 3 assembly sequence.

The uniform geometrical theory of diffraction (GTD) is an effective modeling tool for GPS multipath analysis.[3] Because the GTD technique is computationally intensive, the rigorous multipath computations for a complex vehicle like the space station pose a challenging task. More than 50 basic structural elements, composed of plates and cylinders, are needed for an assembly complete space station model. A volumetric pattern at a 2-deg grid density over the GPS field of view will require considerable computing time. In addition, the solar panels and thermal radiators are not stationary. The solar panels track and thermal radiators antitrack the sun's rays. The space station configuration thus dynamically changes in the time domain. The conventional GTD computer modeling approach requires recalculating the multipath for all space station structural elements at every time step, whenever the solar panels or thermal radiators change their orientations. This approach results in excessive computing time.

A new approach is proposed to investigate the effects of dynamic solar panel and thermal radiator movements on GPS carrier phase measurement. This new approach significantly reduces the required computing time at every time step by separating the dynamic structure elements, such as solar panels and thermal radiators, from the static structure elements, such as modules, the Russian power tower, the centrifuge, and the trusses in the rigorous multipath computations using GTD. The total multipath, at every time step, from the space station structures is then the appropriate combination of multipath from both the dynamic structures and the static structures. The multipath effects from the ISS structures were measured as phase errors in millimeters, which are the differences between the received signal phases with and without the ISS structures in place. The 190.5-mm wavelength λ, at the GPS L1 frequency of 1.575 GHz, corresponds to a 360-deg phase error.

New Approach

The carrier phase errors due to multipath are computed by the following procedure when using the newly proposed GTD approach. First, the carrier phase for all four GPS receiving antennas $(\phi_1, \phi_2, \phi_3, \phi_4)$ in free space without multipath from any space station structures is computed. Next, the carrier phase including multipath from the static and dynamic space station structures for all four antennas $(\phi_1^m, \phi_2^m, \phi_3^m, \phi_4^m)$, where $m = s, d$, is computed. The carrier phase ϕ_i^s is computed by modeling only the space station static structures and is computed only once. The carrier phase ϕ_i^d is computed by modeling only the space station dynamic structures and is computed at each time step, whenever the solar panels or thermal radiators change their orientations. The carrier phase shift due to multipath from the static and dynamic ISS structures is determined by $\Delta\phi_i^m = \phi_i^m - \phi_i$, where $m = s, d$ and $i = 1, 2, 3, 4$. Finally, the carrier phase shift errors from the whole ISS structures for each antenna at each time step are determined by $\Delta\phi_i = \Delta\phi_i^s$ if $|\Delta\phi_i^s| > |\Delta\phi_i^d|$ or $\Delta\phi_i = \Delta\phi_i^d$ if $|\Delta\phi_i^d| > |\Delta\phi_i^s|$.

The signal strength or antenna gain degradation due to multipath is computed by a similar procedure when using the newly proposed GTD approach. First, the signal strength or antenna gain for all four GPS receiving antennas (G_1, G_2, G_3, G_4) in free space without multipath from any space station structures is computed. Next, the signal strength or antenna gain including multipath from the static and dynamic space station structures for all four antennas $(G_1^m, G_2^m, G_3^m, G_4^m)$, where $m = s, d$, is computed. The signal strength G_i^s is computed by modeling only the space station static structures and is computed only once in all time. The signal strength G_i^d is computed by modeling only the space station dynamic structures and is computed at each time step, whenever the solar panels or thermal radiators change their orientations. The antenna gain degradation due to multipath from the static and dynamic ISS structures is determined by $\Delta G_i^m = G_i^m - G_i$, where $m = s, d$ and $i = 1, 2, 3, 4$. Finally, the signal strength including multipath degradation from the whole ISS structures for each antenna at each time step is determined by $G_i^m = G_i^s$ if $|\Delta G_i^s| > |\Delta G_i^d|$ or $G_i^m = G_i^d$ if $|\Delta G_i^d| > |\Delta G_i^s|$.

Results

The accuracy of the results from the new technique is compared with that from using the conventional GTD modeling technique. Figure 2 shows that the computed signal strength (or antenna gain) along a selected satellite path is very similar for both the conventional and new GTD modeling approaches. Almost identical phase shift along a selected satellite path is also observed in Fig. 3. Figure 4 shows that the computed percent coverage for the volumetric antenna gain patterns is very close for both the conventional and new GTD modeling approaches. Figure 5 shows that the computed percent coverage for the volumetric phase shift patterns is only slightly different between the conventional and new GTD modeling approaches. There are significant separations in terms of wavelength between the static structures and the dynamic structures that result in insignificant electromagnetic interactions between them.

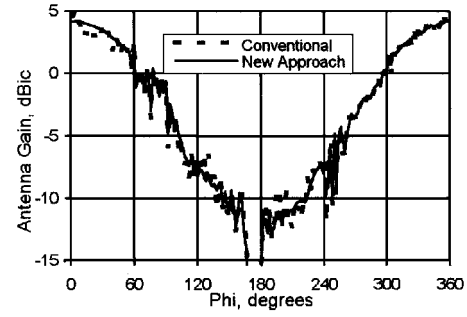

Fig. 2 Signal strength comparison along a satellite path.

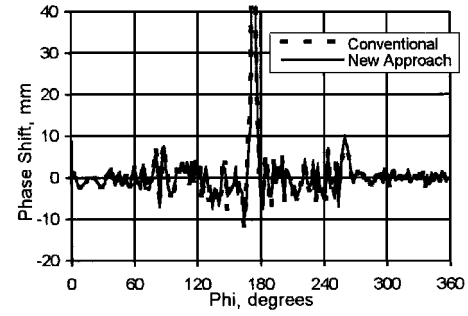

Fig. 3 Phase shift comparison along a satellite path.

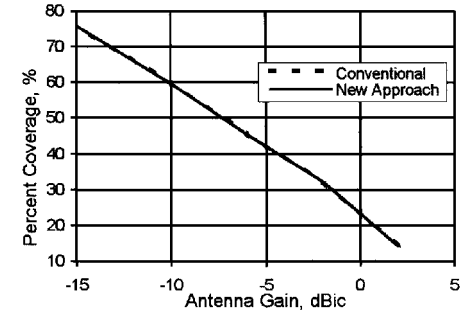

Fig. 4 Comparison for volumetric signal strength pattern.

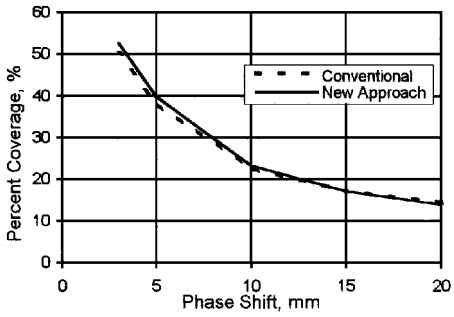

Fig. 5 Comparison for volumetric phase shift pattern.

The difference in the computed antenna gain and phase patterns using the two different modeling approaches is small and is mostly in the small phase shift region (less than 5 mm).

Conclusions

To investigate the effects of dynamic solar panel and thermal radiator movements on the space station GPS carrier phase measurement, a simple approach is proposed. This proposed GTD computer modeling approach is analyzed and compared with the conventional GTD modeling approach for accuracy and efficiency. The proposed new approach, at every time step, recomputes the multipath only from the dynamically changed solar panels and thermal radiators but not from the static structural elements. The total multipath at every time step from the space station structures is then the appropriate combination of multipath from both the changed dynamic structures and the unchanged static structures.

Results obtained from this study indicate this new modeling approach reduces the computing time considerably and only very slightly decreases the accuracy of the percent coverage of the GPS receiver antenna gain and phase shift patterns. This new modeling approach reduces multipath computing time by more than 30%, which is dependent on the actual structure configuration, by ignoring the insignificant electromagnetic interactions between the static structures and the dynamic structures.

References

[1]Cohen, C. E., "Attitude Determination Using GPS," Ph.D. Dissertation, Aeronautics and Astronautics Dept., Stanford Univ., Stanford, CA, Dec. 1992.

[2]Braasch, M., "On the Characterization of Multipath Errors in Satellite-Based Precision Approach and Landing System," Ph.D. Dissertation, Electrical Engineering Dept., Ohio Univ., Athens, OH, June 1992.

[3]Gomez, S. F., Panneton, R. J., Saunders, P. E., Hwu, S. U., and Lu, B. P., "GPS Multipath Modeling and Verification Using Geometrical Theory of Diffraction," *Proceedings of ION GPS-95*, Inst. of Navigation, Alexandria, VA, 1995, pp. 195–204.

A. C. Tribble
Associate Editor